Preparation and Thermal Properties of Resole-Type Phenol Resin–Clay Nanocomposites

Makoto Kato,[1] Azusa Tsukigase,[1] Arimitsu Usuki,[1] Toshihisa Shimo,[2] Hidemi Yazawa[3]

[1]*Organic Materials Laboratory, Toyota Central R&D Labs., Inc. Nagakute, Aichi 480-1192, Japan*
[2]*Toyota Industries Corporation, Kyowa, Obu, Aichi 474-8601, Japan*
[3]*Sumitomo Bakelite Co., Ltd., Fujieda, Shizuoka 426-0041, Japan*

Received 14 June 2005; accepted 5 August 2005
DOI 10.1002/app.22850
Published online in Wiley InterScience (www.interscience.wiley.com).

ABSTRACT: Resole-type phenol resin–clay nanocomposites have been prepared successfully by melt compounding phenol resin with organophilic clay. In the resulting phenol resin–clay nanocomposite, the silicate layers of the clay were exfoliated and dispersed as monolayers. The nanocomposite exhibited higher long-term heat resistance when compared with unmodified phenol resin. It was surmised that the silicate layers of the clay acted as barriers to oxygen penetration into the resin, as the degree of heat degradation of the nanocomposite was much lower than that of the straight phenol resin. © 2006 Wiley Periodicals, Inc. J Appl Polym Sci 99: 3236–3240, 2006

Key words: thermosets; plastics; organoclay; nanocomposites; TEM

INTRODUCTION

A clay mineral is a potential nanoscale additive because it comprises silicate layers in which the fundamental unit is a 1-nm-thick planar structure. If nanometer-scale dispersion of these silicate layers in a polymer matrix could be achieved, the interfacial area might be larger (>700 m^2/g of clay mineral) than that of micrometer dispersions, and the interaction between the silicate layers and the polymer might be maximized. Mechanical properties might also be improved and/or new unexpected hybrid properties derived synergistically under these conditions from the two components. In our previous work, we synthesized a nylon-6–clay hybrid (NCH, the first polymer–clay nanocomposite) in which 1-nm-thick silicate layers of clay minerals were exfoliated and homogeneously dispersed in a nylon 6 matrix.[1] The NCH exhibited various superior properties such as high strength, high modulus, and high heat resistance, compared with conventional nylon 6.[2] Since then, polymer–clay nanocomposites have attracted great research interest, and other polymer–clay hybrids containing polymers such as polyimide,[3] epoxy resin,[4–8] polystyrene,[9–13] polycaprolactone,[14] acrylic polymer,[15] polyurethane,[16] poly(ethylene terephthalate),[17] polypropylene,[18–21] and polyethylene[22] have been reported.

Correspondence to: M. Kato (makoto@mosk.tytlabs.co.jp).

Journal of Applied Polymer Science, Vol. 99, 3236–3240 (2006)

Phenol resin is a thermosetting resin, as is epoxy resin. However, phenol resin–clay nanocomposites have not been investigated much, although a great deal of research has been conducted on epoxy resin–clay nanocomposites. Recently, novolac-type phenol–clay nanocomposites were studied using various organophilic and pristine clays (inorganic clay), with hexamethylenetetramine as a curing agent.[23] However, clay nanocomposites with resole-type phenol resin—that is, the self-curing type (not require curing agent—have not been explored. There were two purposes of this research: first, to prepare resole-type phenol–clay nanocomposites with nanometer-level dispersion of silicate layers in the matrix; and second, to clarify the "nano" effect on the mechanical and thermal properties of phenol resin–clay nanocomposites.

EXPERIMENTAL

Materials

Three types of organophilic clay were used for the investigation of resole-type phenol resin–clay nanocomposites: octadecyl ammonium modified montmorillonite (ODA-Mt), dodecyl ammonium modified montmorillonite (DDA-Mt), and benzyloctadecyldimethyl ammonium modified montmorillonite (BDO-Mt). These organophilic clays were prepared by ion exchange reactions between organic modifiers (aliphatic ammonium ion or aromatic ammonium ions) and Na-montmorillonite. Organic modifiers were obtained from Wako Pure Chemical Industries, Ltd.

TABLE I
Compositions (g) of Nanocomposites Based on Resole-Type Phenol Resin and Organophilic Clay, and the Control

Sample	Resole-type phenol resin	Organophilic clay			Glass fiber	Carbon black
		ODA-Mt	DDA-Mt	BDO-Mt		
Nanocomposite 1	45	7.1 (5)	—	—	40	10
Nanocomposite 2	45	—	6.2 (5)	—	40	10
Nanocomposite 3	45	—	—	7.6 (5)	40	10
Control	45	—	—	—	40	15

The amount of inorganic content of organophilic clay is shown in parentheses.

(Osaka, Japan). Na-montmorillonite (Kunipia F) was obtained from Kunimine Industries Co., Ltd. (Tokyo, Japan), with a cationic exchange capacity of 115 meq/100 g. The inorganic contents of ODA-Mt, DDA-Mt, and BDO-Mt were 70.1, 81.1, and 65.7 wt %, respectively. The *d*-spacings of ODA-Mt, DDA-Mt, and BDO-Mt were 2.03, 1.88, and 2.62 nm, respectively, obtained by X-ray diffraction (XRD) measurements of the (001) face.

Resole-type phenol resin (Sumikon PM) was obtained from Sumitomo Bakelite Co., Ltd. (Tokyo, Japan). This phenol resin was solid type and the molecular weight was 2000–5000 by GPC method.

Glass fiber and carbon black were used as other materials. The fiber diameter of the glass fiber was 11 μm on an average. The fiber length of the glass fiber was 150–200 μm on an average after compression molding. The diameter of carbon black was 24 nm on an average.

Preparation of resole-type phenol resin–clay nanocomposites

Initially, each organophilic clay was mixed with phenol resin using a kneading roller. About 5 wt % (as inorganic content) of clay was added, as shown in Table I. Dry blended powders of phenol resin, organophilic clay, glass fiber, and carbon black were added to a hot kneading roller. The kneading temperature was 80–90°C, which allowed the mixture to undergo an intercalation reaction, because the phenol resin was changed from a solid state to a liquid state. The kneaded materials were cooled and granulated by a disintegrating machine. Test pieces for evaluating the dispersibility of the clays in the phenol resin matrix and for measuring mechanical and thermal properties were prepared from these powders by compression molding, details of which are described in the following section.

Evaluation of the dispersibility of the clays in a phenol resin matrix

The dispersibility of silicate layers in the phenol resin–clay nanocomposites was evaluated by using an X-ray diffractometer and a transmission electron micrograph (TEM). XRD patterns of phenol resin–clay nanocomposite sheets and related samples were obtained with a Rigaku RAD-B X-ray diffractometer, using Cu Kα radiation at 30 kV and 30 mA. TEM observations of the hybrids were performed on ultrathin sections of the sheets using a JEM-2010 TEM with an acceleration voltage of 200 kV. The test pieces were 1 mm thick and 120 $\times$ 120 mm^2. The molding conditions were as follows: the molding temperature was 175°C, the curing time was 3 min, the compacting pressure was 15 MPa, and the mold clamping force of the compression molding machine was 343 kN. Test pieces of a suitable size were cut out from the molded samples and used for measurements.

Measurement of mechanical properties and heat resistance

The flexural property of phenol resin–clay nanocomposites was measured at 23°C according to ISO 178 using an INSTRON universal materials testing system (type 4302). The speed of the crosshead was 5 mm/min. Five separate measurements were determined, which were averaged to obtain a value for the flexural property. Test pieces (10 $\times$ 80 mm^2 hexahedra with a thickness of 4 mm) for the flexural test were obtained by compression-molding using the same conditions as in the previous section.

Heat resistance properties of the nanocomposites were evaluated by the following method. The test pieces were kept at 200°C in a dry oven and removed at fixed intervals for flexural strength measurements. Strength retention was calculated and compared with initial flexural strength. Strength retention of nanocomposites and of controls was evaluated as a function of time.

EPMA analysis of oxygen distribution of nanocomposites

To clarify the influence of oxidation on nanocomposites by the heat resistance test, nanocomposites and control samples were analyzed for oxygen atom distribution using electron probe microanalysis (EPMA).

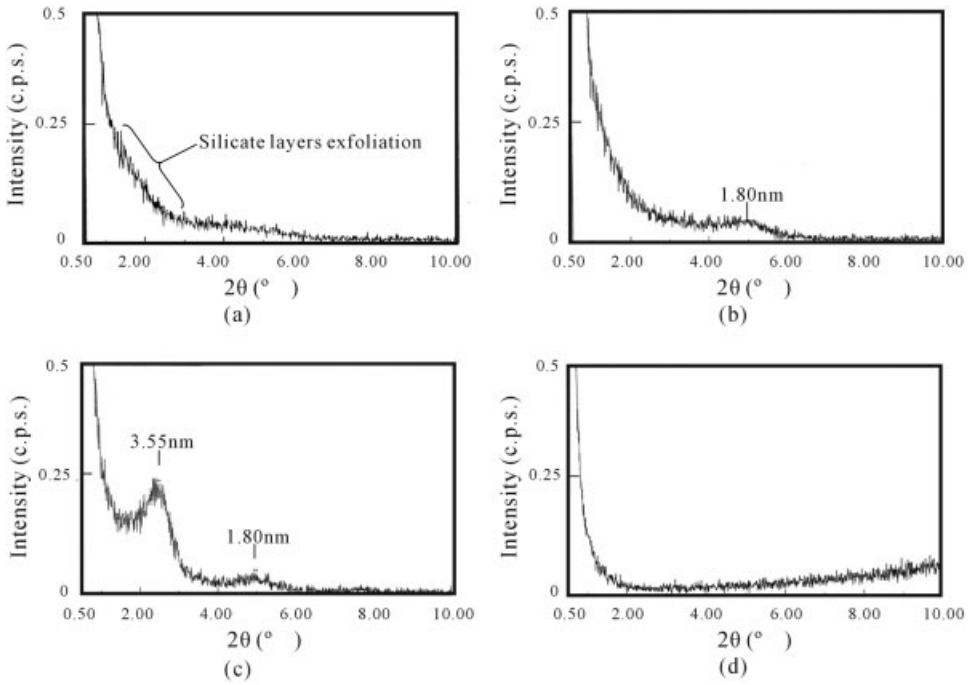

Figure 1 XRD patterns of the phenol–clay nanocomposites and control: (a) Nanocomposite 1 (ODA-Mt), (b) Nanocomposite 2 (DDA-Mt), (c) Nanocomposite 3 (BDO-Mt), (d) Control (blank).

Depth profiles of oxygen atom distribution were obtained using linear analysis and element mapping by scanning cross sections of these samples. EPMA analysis data were obtained using a Shimadzu model 810Q EPMA apparatus.

RESULTS AND DISCUSSION

Evaluation of the dispersibility of the clay layers in the nanocomposites

Direct evidence of the nanometer-scale dispersion of the silicate layers of the clay was provided by the XRD patterns of the nanocomposites (Fig. 1). The XRD pattern of the phenol resin nanocomposite containing ODA-Mt is shown in Figure 1(a), which does not contain a diffraction peak from the (001) face of ODA-Mt. The diffraction strength (signal intensity) of this sample gradually decreased from low to high angle. In contrast, the signal intensity of the blank XRD pattern, shown in Figure 1(d), decreased rapidly (not gradually) until the angle was 1°, after which it showed a slight rise in intensity as 2θ approaches 10°, showing that there was nothing from which X-rays were reflected. These results indicate that the interlayer distance of silicate layers in the sample containing ODA-Mt was expanded beyond 10 nm on average. NCH, containing completely dispersed silicate layers in a nylon 6 matrix, had no peak but exhibited a gradual decrease in XRD signal strength between 0.5 and 10°. Therefore, nanometer-scale dispersion of silicate layers was similarly achieved in the resole-type phenol resin matrix. The XRD pattern of the phenol resin nanocomposite containing DDA-Mt is shown in Figure 1(b), in which a shoulder peak indicated a distance of 1.8 nm between silicate layers. Because the *d*-spacing of DDA-Mt itself is 1.88 nm, this peak was thought

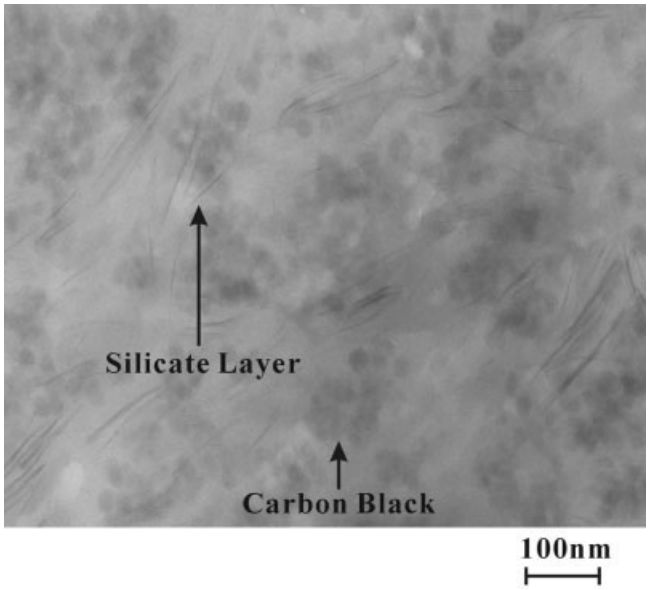

Figure 2 Transmission electron micrograph of the phenol–clay nanocomposite. The dark lines are cross sections of the silicate layers. The aggregated particles are carbon black.

TABLE II
Flexural Properties of Nanocomposite and the Control

Sample	Strength		Modulus		Distortion at break	
	MPa	Std	GPa	Std	%	Std
Nanocomposite 1 (ODA-Mt)	140	3	11.3	0.6	1.4	0.1
Control	201	7	11.6	0.6	1.9	0.1

to show that DDA-Mt was slightly more incompatible with the resin matrix in comparison with ODA-Mt. The XRD pattern of the phenol resin nanocomposite containing BDO-Mt is shown in Figure 1(c), which displayed two peaks, indicating distances of 3.55 and 1.80 nm, respectively, between the silicate layers. These peaks were distinct from the *d*-spacing of BDO-Mt, and it was thought that the resole-type phenol resin inserted itself between the layers.

To confirm the dispersibility of the silicate layers in the ODA-Mt-containing nanocomposite, which had the best dispersibility of these samples, the silicate layers were studied using TEM. A TEM micrograph of this sample is shown in Figure 2, where the dark lines are cross sections of the silicate layers (1 nm thickness) in the clay. The silicate layers were dispersed homogeneously in the resole-type phenol resin matrix. From these results we concluded that a resole-type phenol resin–clay nanocomposite could be produced using ODA-Mt.

Mechanical and heat resistance properties of the phenol resin–clay nanocomposite

The mechanical properties of the phenol resin–clay nanocomposite containing ODA-Mt, and of a control sample without clay are summarized in Table II. The flexural modulus of this nanocomposite was almost the same as that of the control sample, but its flexural strength was lower than the control sample's. Thus, the "nano" effect was not discernible in the straightforward mechanical properties. However, this effect was apparent in the heat resistance properties. The retention of flexural strength after heat degradation is shown in Figure 3. The retention of flexural strength by this nanocomposite at 500 and 1000 h was significantly higher than that of the control, and the reason for this improvement is discussed hereunder.

Depth profiles of oxygen atom distribution in the ODA-Mt-containing nanocomposite as a function of exposure time are shown in Figure 4, along with profiles of a control sample. In the control sample, oxygen atoms originating from oxidation reached the center of the test piece by 1000 h. In the nanocomposite, however, these oxygen atoms were distributed to a depth of about 600 nm at 1000 h. Although at 2000 h the oxygen atoms reached the center of the nanocomposite test piece as well, this degree of heat resistance is remarkable. The oxygen atom distribution at 1000 h obtained by element mapping in the nanocomposite is shown in Figure 5. Because of the presence of glass fibers in this nanocomposite, the distribution of silicon atoms from the fibers was also examined. The purpose of this was to distinguish between oxygen originating from oxidation and oxygen of the glass fiber. Oxygen atoms from oxidation were distributed to a depth

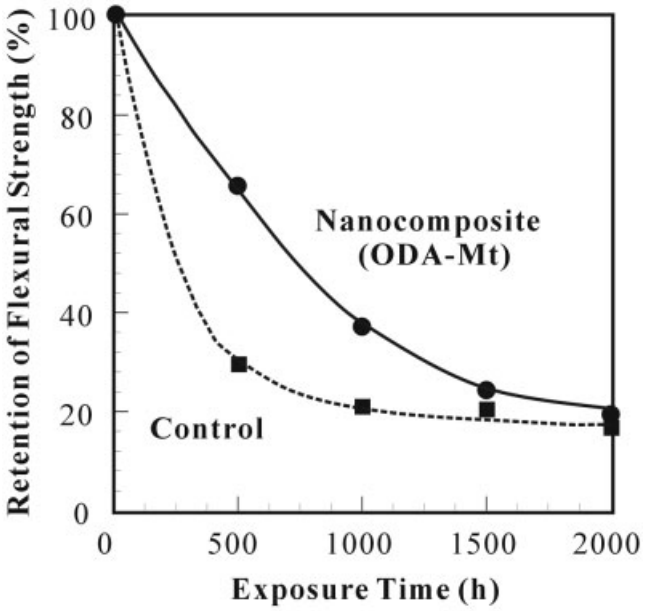

Figure 3 Retention of flexural strength after heat-resistance test at 200°C.

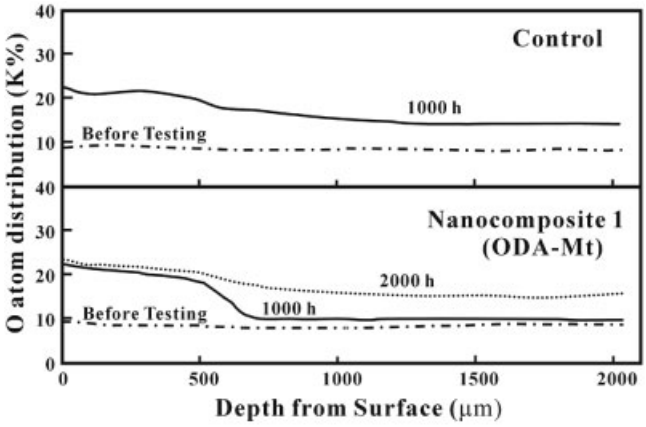

Figure 4 Depth profile of O atom distribution after heat-resistance test at 200°C. K% is the relative intensity of X-rays of the sample to that of targeted element 100%.

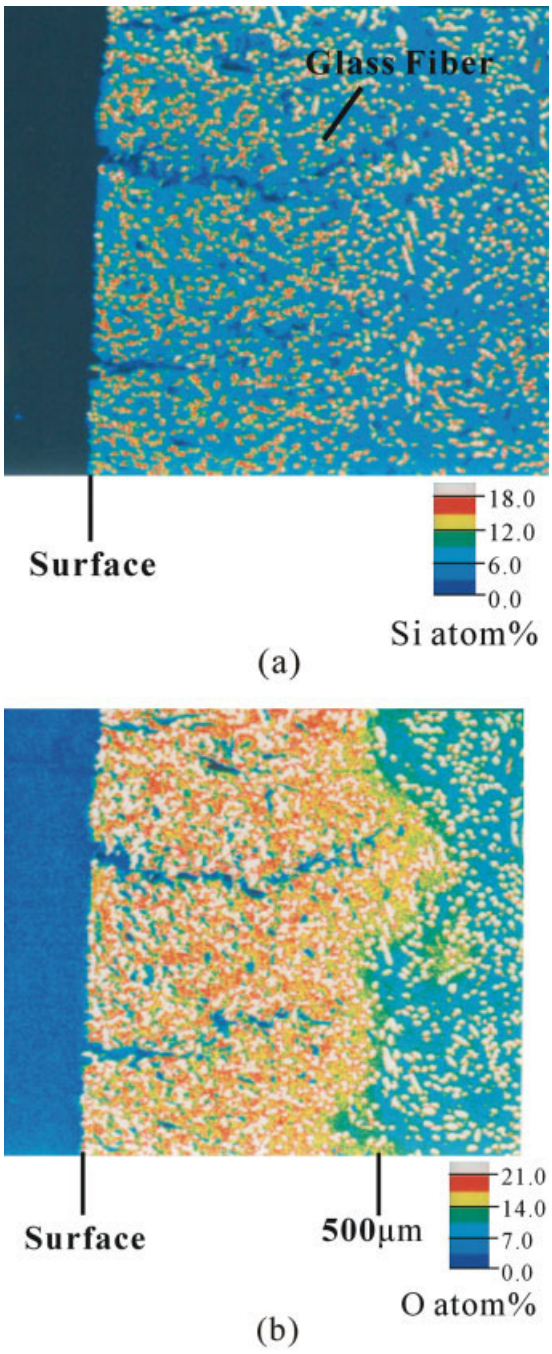

Figure 5 Depth profile of Si and O atom distribution (element mapping) of Nanocomposite 1 (ODA-Mt) after heat-resistance test at 200°C, 1000 h: (a) Si atom distribution, originating from glass fibers. (b) O atom distiribution. [Color figure can be viewed in the online issue, which is available at www.interscience.wiley.com.]

about 500–600 nm, but not deeper. Thus, the nanocomposite exhibited excellent heat resistance because oxidation was inhibited.

The reason for the foregoing conclusion regarding heat resistance is as follows. In general, nanocomposites are expected to possess significant gas barrier properties, because the gas must bypass silicate layers distributed homogeneously in a matrix. In this study, the heat resistance of this nanocomposite depended on its oxidation resistance, as shown earlier. The silicate layers prevented the penetration of oxygen atoms into the nanocomposite, conferring excellent heat resistance.

CONCLUSIONS

We have successfully prepared a resole-type phenol resin–clay nanocomposite using octadecyl ammonium modified montmorillonite. In this material, the clay silicate layers were exfoliated and dispersed at the nanometer level in a phenol resin matrix. The resulting phenol resin–clay nanocomposite exhibited superior heat resistance.

References

1. Usuki, A.; Kawasumi, M.; Kojima, Y.; Fukushima, Y.; Okada, A.; Kurauchi, T.; Kamigaito, O. J Mater Res 1993, 8, 1179.
2. Kojima, Y.; Usuki, A.; Kawasumi, M.; Fukushima, Y.; Okada A.; Kurauchi, T.; Kamigaito, O. J Mater Res 1993, 8, 1185.
3. Yano, K.; Usuki, A.; Okada, A.; Kurauchi, T. J Polym Sci Part A: Polym Chem Ed 1993, 31, 2493.
4. Usuki, A.; Mizutani, T.; Fukushima, Y.; Fujimoto, M.; Fukumori, K.; Kojima, Y.; Sato, N.; Kurauchi, T.; Kamigaito, O. U.S. Pat. 4,889,885 (1989).
5. Wang, M. S.; Pinnavaia, T. J. Chem Mater 1994, 6, 468.
6. Lan, T.; Pinnavaia, T. J. Chem Mater 1994, 6, 2216.
7. Lan, T.; Kaviratona, P. J. Pinnavaia, T. J Chem Mater 1995, 7, 2214.
8. Kelly, P.; Akelah, A.; Qutubuddin, S.; Moet, A. J Mater Sci 1994, 29, 2274.
9. Vaia, R. A.; Isii, H.; Giannelis, E. P. Chem Mater 1993, 5, 1694.
10. Vaia, R. A.; Jandt, K. D.; Edward, J K.; Giannelis, E. P.; Macromolecules 1995, 28, 8080.
11. Weiner, M. W.; Chen, H.; Giannelis, E. P.; Sogah, D. Y. J Am Chem Soc 1999, 122, 1615.
12. Moet, A.; Akelah, A.; Mater Lett 1993, 18, 97.
13. Hasegawa, N.; Okamoto, H.; Kawasumi, M.; Usuki, A.; J Appl Polym Sci 1999, 74, 3359.
14. Messersmith, P.B.; Giannelis, E. P.; J Polym Sci Part A: Polym Chem Ed 1995, 33, 1047.
15. Biasci, L.; Aglietto, M.; Ruggeri, G.; Ciardelli, F. Polymer 1994, 35, 3296.
16. Zilg, C.; Thomann, R.; Mulhaupt, R.; Finter, J. Adv Mater 1999, 11, 49.
17. Ke Y.; Long, C.; Qi, Z. J Appl Polym Sci 1999, 71, 1139.
18. Usuki, A.; Kato, M.; Okada, A.; Kurauchi, T. J Appl Polym Sci 1997, 63, 137.
19. Kato, M.; Usuki, A.; Okada, A.; Kurauchi, T. J Appl Polym Sci 1997, 66, 1791.
20. Kawasumi, M.; Hasegawa, N.; Kato, M.; Usuki, A.; Okada, A.; Macromolecules 1997, 30, 6333.
21. Hasegawa, N.; Kawasumi, M.; Kato, M.; Usuki, A.; Okada, A. J Appl Polym Sci 1998, 67, 87.
22. Kato, M.; Okamoto, H.; Hasegawa, N.; Usuki, A. Polym Eng Sci 2003, 43, 1312.
23. Choi, M. H.; Chung, I. J.; Lee, J. D. Chem Mater 2000, 12, 2977.